Floe size distributions in irregular sea states

Nicolas Mokus, Fabien Montiel
Department of Mathematics and Statistics, University of Otago, Dunedin, New Zealand
nmokus@maths.otago.ac.nz

Highlights

We develop and implement an efficient multiple scattering model to study the wave-induced breakup of sea ice floes. We use it to observe the emergence of a floe size distribution after repeated breakup events. We find the resulting distribution is right-skewed and better approximated by a lognormal model than the often used Pareto model.

1 Introduction

Sea ice is a distinctive feature of both polar oceans. By drastically altering the ocean surface albedo and interrupting the fluxes of matter, kinetic energy, and thermal radiation between oceans and atmosphere, it has an extensive impact on their circulations and the Earth's climate. The marginal ice zone (MIZ) is the transition belt between an ice-free ocean and the pack ice. It features a collection of ice floes of varying sizes, distinguishing it from a continuous ice cover, and is notably affected by waves. The shape of this floe size distribution (FSD) has been an active topic of research for decades [1]. Wave activity is one of the drivers of the FSD evolution which, in turn, controls wave propagation. Smaller floes are more sensible to melt, and lower ice concentration allows waves to propagate further into the MIZ, introducing a positive feedback loop. Therefore, representing the FSD in global climate models is necessary to improve their accuracy and enhance their long-term forecast capabilities.

Remote sensing observation of floe sizes have suggested the FSD follows a Pareto (power law) distribution [1, 2]. This led to its adoption in various modelling studies. However, recent field observations [3, 4], laboratory experiments [5, 6] and numerical models [7, 8] propose contrasting distributions. The role of wave activity in the emergence of the Pareto distribution [3], and even the validity of this statistical model [9, 10], are unclear. In a recent modelling study [11], we combine FSDs obtained under monochromatic forcings to simulate the FSD resulting from a wave spectrum. We find the lognormal distribution is a strong parametric alternative to the Pareto distribution. In this abstract, we show that this model is also appropriate for the FSD produced by repeated breakup under polychromatic wave forcing.

2 Mathematical model

2.1 Wave scattering

Our model is based on linear water wave theory. We consider the scattering of surface gravity waves propagating in the x direction, in a two-dimensional fluid domain of constant depth H, by an array of ice floes modelled as visco-elastic floating plates [12] with free edge boundary conditions. Floes are non-overlapping so that individual floes are separated by open water, delimiting homogeneous sub-domains. Floe j is identified by the coordinate of its left edge, x_j, and its length, L_j. This geometry is illustrated on Figure 1. The fluid velocity derives from a

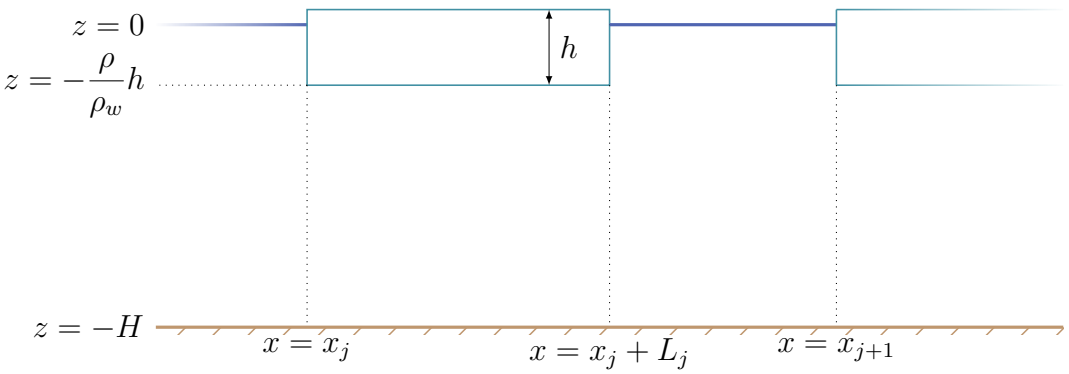

Figure 1: Geometry of the model at rest.

scalar, time-harmonic potential Φ solution of Laplace's equation. We further assume separation of space and time variables so that $\Phi = \mathrm{Re}\left[\phi\left(x,z\right)\exp(-i\omega t)\right]$ with ω a prescribed angular frequency. We note g the acceleration of gravity, D the floes flexural rigidity, h their thickness, ρ their density, γ their viscosity, ρ_w the fluid density. The ensuing boundary conditions on the fluid top surface and at the impervious seabed lead to the dispersion relations

$$k\tanh\left(kH\right) = \frac{\omega^2}{g} \quad ; \quad \left(\frac{D}{\rho_w g}k^4 + 1 - \frac{\omega^2}{g}\frac{\rho}{\rho_w}h - i\frac{\gamma\omega}{\rho_w g}\right)k\tanh\left(k\left(H - \frac{\rho}{\rho_w}h\right)\right) = \frac{\omega^2}{g} \tag{1}$$

with respective roots k^w and k^f in respectively open water and ice-covered sub-domains.

The potential ϕ is expanded onto these wave modes in every sub-domain, and the expansion coefficients are determined to ensure continuity of pressure and velocity across the horizontal interfaces between adjacent sub-domains. It fully determines the spatial part of Φ in the whole domain. More details on the solution method can be found in [11].

2.2 Breakup parametrisation

Strain is often used to parametrise wave-induced breakup [13]. Here, we consider the maximum strain undergone by each floes. We use the plane stress approximation so that for a given ice floe, this maximum strain, in absolute value, is located on either top or bottom surface of the floe. The motion of the bottom surface is derived from the wave field, fully characterised by ϕ, so that

$$\tilde{\varepsilon}\left(x,\omega\right) = \frac{h}{2\omega}\left|\mathrm{Re}\left[i\frac{\partial^2}{\partial x'^2}\frac{\partial\phi}{\partial z}\right]\right|. \tag{2}$$

Our model solves for the scattering of a monochromatic wave. The strain field undergone by the floes is a consequence of this monochromatic forcing. To estimate the strain field resulting from a developed sea, we introduce the theoretical Pierson-Moskowitz spectrum

$$S(\omega) = c_1\frac{g^2}{\omega^5}\exp\left(-c_2\frac{g^2}{\omega^4 {H_s}^2}\right) \tag{3}$$

where $c_1 = 8.1\times10^{-3}$, $c_2 = 3.24\times10^{-2}$ are non-dimensional constants. This spectrum is parametrised by the significant wave height $H_s = 4\sqrt{\int_0^{+\infty}S(\omega)\mathrm{d}\omega}$. Using the superposition principle, the strain under such a forcing can be written as

$$\varepsilon(x) = \frac{\int_{\omega_{\min}}^{\omega_{\max}}\tilde{\varepsilon}(x,\omega)S(\omega)\mathrm{d}\omega}{\int_{\omega_{\min}}^{\omega_{\max}}S(\omega)\mathrm{d}\omega} \tag{4}$$

where the bounds $\omega_{\min}, \omega_{\max}$ are used for numerical integration, ensuring we capture a significant part of the spectrum, Equation (4) being evaluated on 200 equally spaced angular frequencies.

As in [11], we set floe j to break when $\max_{x' \in [0, L_j]} \varepsilon_j(x') > \varepsilon_c$ where ε_c is an empirically determined strain threshold. We situate the breakup point at $x_b = \text{argmax}\ \varepsilon_j$ so that a floe of length L_j breaks into two floes of length x_b and $L_j - x_b$.

2.3 Numerical experiment

Our experiment is summarised by the following steps:

1. The domain is initialised with a single, semi-infinite floe.
2. The scattered wave field is determined for 200 frequencies between $\omega_{\min}$ and $\omega_{\max}$.
3. The ensuing strain field is derived from Equation 4. All floes meeting the breakup condition are split and the domain updated.
4. Steps 2 and 3 are repeated until none of the floes break.
5. The resulting finite lengths are recorded.

To account for wave dispersion, at each iteration individual waves are assigned a phase sampled uniformly in $[0, 2\pi)$. Additionally, after every breakup event floes are assigned random new locations, preserving their order, to enforce they do not overlap. These sources of randomness impact the resulting FSD. Therefore, we run the same simulation several times, to obtain an ensemble of FSDs.

3 Preliminary results and conclusions

We investigate the behaviour of the model under small-amplitude wave forcing, setting $H_s = 1\,\text{m}$. The ice properties are set to $h = 1\,\text{m}$, $\gamma = 20\,\text{Pa}\,\text{s}\,\text{m}^{-1}$, $\varepsilon_c = 4 \times 10^{-5}$. The resulting distributions are right-skewed. We average them over 40 model realisations. Specifically, these 40 sets of floe lengths are assembled into a single dataset, which is equivalent to averaging count histograms computed on the same bins. We estimate, by maximum likelihood, parameters for a Pareto distribution (following a common assumption in wave–sea ice modelling) and for a lognormal distribution. In Figure 2, we compare these parametric distributions to a kernel density estimate of the FSD.

Even though the lognormal distribution does not perfectly fit the data, especially for larger floe lengths, it is a better match than the Pareto distribution. The predicted mode of a Pareto distribution is the smallest admissible floe size, while our empirical distribution clearly is not monotonic. This reinforces our recent modelling findings [11] and suggest a reappraisal of the de facto power law assumption adopted in the modelling community [14, 15].

The polychromatic parametrisation used here differs from the one used in [11]. The results are qualitatively similar but differ quantitatively, as shown in Figure 2. It is not clear which one of these parametrisations has more physical significance. Additional observational data is needed to confirm or invalidate these statistical models. We do not attempt at this stage to evaluate the impact of empirical parameters such as ε_c or γ on these results. This will be discussed during the presentation.

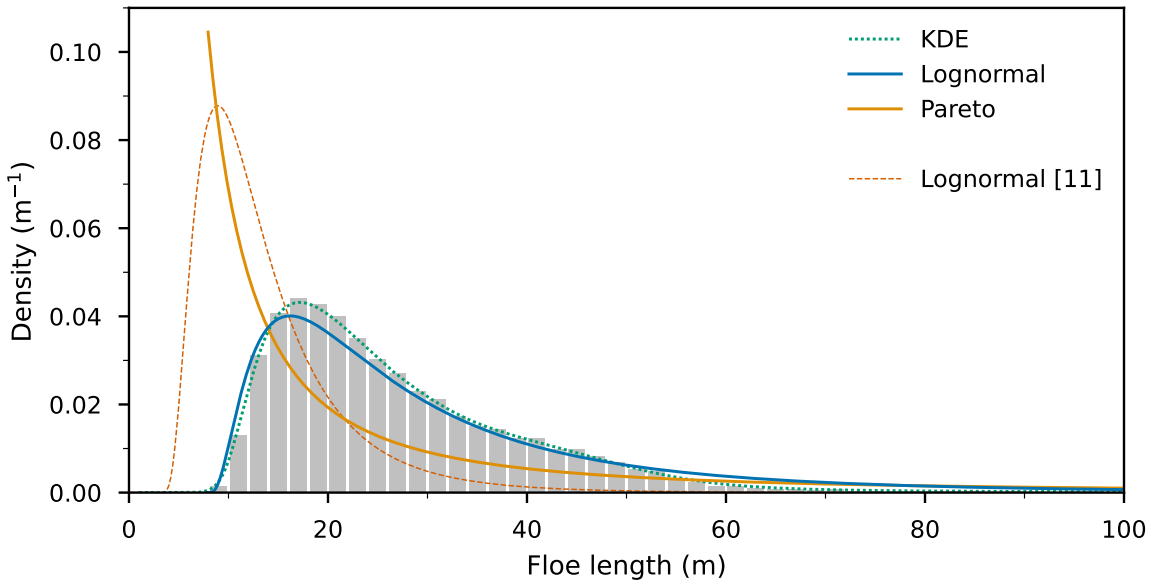

Figure 2: Average FSD over 40 model realisations. Two non-parametric density estimates (histogram, kernel density) are compared to two parametric models. The histogram bin width is 2 m. The lognormal fit to a similar configuration, obtain by combining monochromatic FSDs [11], is added for comparison.

REFERENCES

[1] Rothrock, D. A., and Thorndike, A. S. 1984. *Measuring the sea ice floe size distribution.* Journal of Geophysical Research 89(C4), 6477.

[2] Toyota, T., Takatsuji, S., and Nakayama, M. 2006. *Characteristics of sea ice floe size distribution in the seasonal ice zone.* Geophysical Research Letters 33(2).

[3] Herman, A., Wenta, M., and Cheng, S. May 2021. *Sizes and Shapes of Sea Ice Floes Broken by Waves–A Case Study From the East Antarctic Coast. Frontiers in Earth Science 9*.

[4] Dumas-Lefebvre, E., and Dumont, D. 2021. *Aerial observations of sea ice break-up by ship waves. The Cryosphere Discussions 2021*, 1–26.

[5] Dolatshah, A., Nelli, F., Bennetts, L. G., Alberello, A., Meylan, M. H., Monty, J. P., and Toffoli, A. Sept. 2018. *Letter: Hydroelastic interactions between water waves and floating freshwater ice.* Physics of Fluids 30(9), 091702.

[6] Herman, A., Evers, K.-U., and Reimer, N. Feb. 2018. *Floe-size distributions in laboratory ice broken by waves.* The Cryosphere 12(2), 685–699.

[7] Montiel, F., and Squire, V. A. Oct. 2017. *Modelling wave-induced sea ice break-up in the marginal ice zone.* Proceedings of the Royal Society A: Mathematical, Physical and Engineering Science 473(2206), 20170258.

[8] Herman, A. Nov. 2017. *Wave-induced stress and breaking of sea ice in a coupled hydrodynamic discrete-element wave–ice model.* The Cryosphere 11(6), 2711–2725.

[9] Clauset, A., Shalizi, C. R., and Newman, M. E. J. Nov. 2009. *Power-Law Distributions in Empirical Data.* SIAM Review 51(4), 661–703.

[10] Stern, H. L., Schweiger, A. J., Zhang, J., and Steele, M. Jan. 2018. *On reconciling disparate studies of the sea-ice floe size distribution. Elementa: Science of the Anthropocene 6*.

[11] Mokus, N. G. A., and Montiel, F. 2021. *Wave-triggered breakup in the marginal ice zone generates lognormal floe size distributions. The Cryosphere Discussions 2021*, 1–33.

[12] Robinson, N., and Palmer, S. Nov. 1990. *A modal analysis of a rectangular plate floating on an incompressible liquid.* Journal of Sound and Vibration 142(3), 453–460.

[13] Kohout, A. L., and Meylan, M. H. Sept. 2008. *An elastic plate model for wave attenuation and ice floe breaking in the marginal ice zone.* Journal of Geophysical Research 113(C9).

[14] Williams, T. D., Bennetts, L. G., Squire, V. A., Dumont, D., and Bertino, L. Nov. 2013. *Wave–ice interactions in the marginal ice zone. Part 1: Theoretical foundations. Ocean Modelling 71*, 81–91.

[15] Boutin, G., Lique, C., Ardhuin, F., Rousset, C., Talandier, C., Accensi, M., and Girard-Ardhuin, F. Mar. 2020. *Towards a coupled model to investigate wave–sea ice interactions in the Arctic marginal ice zone.* The Cryosphere 14(2), 709–735.